

One-step Fabrication of Sharp Platinum/Iridium Tips via Amplitude-Modulated Alternating-Current Electropolishing

Y. Nishiwaki, T. Utsunomiya, S. Kurokawa, and T. Ichii*

*Department of Materials Science and Engineering, Kyoto University,
Yoshida Honmachi, Sakyo, Kyoto, 606-8501, Japan.*

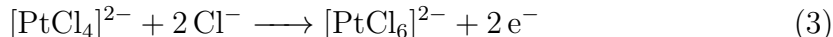
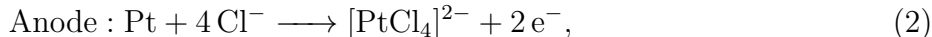
(*Electronic mail: ichii.takashi.2m@kyoto-u.ac.jp)

(Dated: 3 December 2024)

The platinum/iridium (Pt/Ir) alloy tip for scanning probe microscopy (SPM) was successfully fabricated by amplitude-modulated alternating-current (AC) electropolishing. The clean tips with a radius of curvature less than 100 nm were reproducibly obtained by applying the 1000 Hz sinusoidal voltage with amplitude modulation of the sinusoidal wave of 100 Hz in $\text{CaCl}_2/\text{H}_2\text{O}/\text{acetone}$ solution. The analyses by scanning electron microscopy with an energy-dispersive X-ray analyzer (SEM-EDX) and atom probe tomography (APT) showed that a uniform Pt/Ir alloy was exposed on the tip surface as a clean surface without O or Cl contamination. The STM imaging using the fabricated tip showed that it is more suitable for investigating rough surfaces than conventional as-cut tips and applicable for atomic-resolution imaging. Furthermore, we applied the fabricated tip to qPlus AFM analysis in liquid and showed that it has atomic resolution in both the horizontal and vertical directions. Therefore, it is concluded that the amplitude-modulated AC etching method reproducibly provides sharp STM/AFM tips capable of both atomic resolution and large-area analyses without complex etching setups.

A platinum/iridium (Pt/Ir) alloy tip is widely used in scanning probe microscopy (SPM) because it has high mechanical strength and chemical stability, and an adequately sharp cut end can be easily obtained by mechanical cutting.¹⁻³ In particular, mechanically cut Pt/Ir tips are the first choice for high-resolution scanning tunneling microscopy (STM)⁴ in ambient air, requiring a tip that does not react with air and is highly strong.^{2,3} However, the tip shape of the mechanically cut wire is not reproducible³ and often produces image artifacts, such as multiple-tip effects.⁵⁻⁷ Therefore, a method to fabricate a sharp Pt/Ir tip with a controlled shape and high reproducibility is demanded. Electropolishing is a low-cost and quick method for fabricating SPM tips.^{8,9} Pt/Ir wires can be electropolished by the alternating-current (AC) electrolysis technique in CaCl_2 ^{3,10,11} or KCl ¹² aqueous solution, typically at an AC voltage of $10 V_{\text{rms}}$ or higher¹². However, it is known to be difficult to obtain sufficiently sharp tips by this method; therefore, additional complex techniques, such as upside-down electrolytic baths (reversed-etching)^{7,13,14} or multi-step etching with different electrolytes^{10,15} and applied voltages^{14,16,17}, are often used together. The reversed-etching method is typically performed by inserting a wire from below into an electrolyte supported by a glass pipette,¹⁴ which requires a precise positioning technique combined with a high-quality vibration-isolation system.¹⁴ Also, in the multi-step techniques, the tip shape strongly depends on the position of the tip on the solution surface and when to stop the first-step etching and proceed to the following step, which depends on the operator's skills. Therefore, the reproducible electropolishing method for fabricating sharp Pt/Ir tips without a complex setup or procedure has been required.

AC electropolishing of Pt in the presence of Cl^- ions is explained by the oxidation of Pt and the mechanical removal of deposits on the tip surface by gas bubbles generated by the counter-reaction, as described by the following reaction formulas:¹⁸



During the reactions (2) and (3), PtO_x is produced as an intermediate¹⁸, which would lead to the formation of an oxide film on the tip surface. Also, $[\text{PtCl}_4]^{2-}$ and $[\text{PtCl}_6]^{2-}$ ions produced in the anodic reaction are easily precipitated as Pt particles or platinum chloride PtCl_x ¹² and often contaminate the tip surface. Therefore, mechanical exfoliation and flushing of

these deposits from the tip surface by the electrochemically-generated gas bubbles plays a crucial role in the etching procedure as well as the anodization of Pt. However, the flushing rate by gas bubbles is usually insufficient against the anodization rate of Pt. Hence, a tip with an irregular shape and contamination on the surface is often produced in conventional AC etching.

To overcome this issue, we propose an approach that increases the generation rate of the gas bubbles against the anodization rate of Pt by modulating the amplitude of the AC voltage applied between the wire and the counter electrode. This approach is based on the fact that the oxidation of Pt does not proceed at voltages below $10 V_{\text{rms}}$, and alternatively, only the generation of H_2 gas in equation (1) and the generation of Cl_2 gas expressed in the following equation¹⁹ proceed.



By modulating the amplitude of the applied voltage in AC electrolysis across $10 V_{\text{rms}}$, the etching reaction with Pt oxidation and H_2 gas generation above $10 V_{\text{rms}}$ and the gas bubble generation of H_2 and Cl_2 without Pt anodization below $10 V_{\text{rms}}$ are periodically repeated. Note that flushing with low-voltage-generated gases is commonly used as an independent step in the multi-step method to clean the tip surface after AC etching.¹⁷ However, deposits produced during the etching affect the etching process and make the tip shape irregular. Therefore, removal of deposits by flushing after the etching process is not sufficient, and it is important to repeatedly remove the deposits by gas bubbles during the etching process. Hence, the amplitude-modulation method is more straightforward than the conventional multi-step method and has the potential to produce sharper and cleaner tips than the multi-step method. In order to clarify whether this method can fabricate clean and sharp tips as opposed to conventional constant-amplitude AC electropolishing, we investigated the shape and chemical composition of the fabricated tips by scanning electron microscopy with energy-dispersive X-ray analyzer (SEM-EDX) and atom probe tomography (APT)²⁰. Furthermore, to evaluate the suitability for the various SPM analyses, we applied the fabricated tip to STM in air and atomic force microscopy (AFM)²¹ in liquid and compared it with a conventional mechanically cut tip.

The experimental procedure was as follows. The acetone-saturated CaCl_2 solution proposed by Libioulle *et al.*¹⁰ was used as the electrolyte solution. 40 mL of ultrapure water

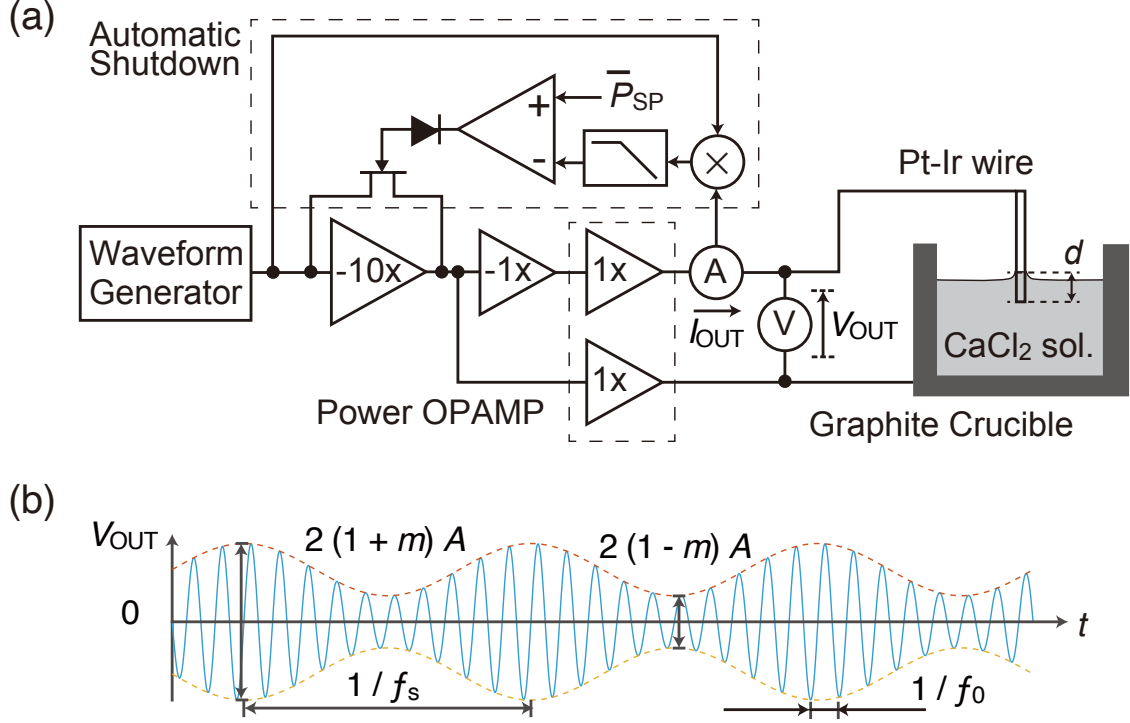


FIG. 1. (a) The block diagram of the setup for amplitude-modulated AC etching. (b) An ideal waveform of the voltage applied to the cell V_{OUT} versus time t .

(UPW, $>18.2 \text{ M}\Omega \text{ m}^{-1}$) and 40 mL of acetone ($>99.5 \%$, Nacalai Tesque Inc.) were mixed thoroughly, and 14 g of CaCl_2 anhydride ($>95.0 \%$, Nacalai Tesque Inc.) was added to the mixture. When CaCl_2 was added, the mixture spontaneously separated into two layers, and the water-rich lower layer (namely acetone-saturated CaCl_2 aqueous solution) was pipetted out and used as the electrolyte solution. 10 mL of the electrolyte solution was poured into a 25 mL graphite crucible, which was used as a counter electrode and a reaction cell. The platinum-iridium wire (Pt 80 wt% - Ir 20 wt%, Nilaco Corp.) with a diameter of 0.1 mm was immersed in the electrolyte at a depth of ~ 1 mm utilizing the wire holder of commercial tungsten STM tip etcher (UTE-1001; Unisoku Inc.), which provides coarse positioning of the tip and the electrical connection to the tip. The amplitude-modulated voltage was generated by a waveform generator (AFG3022B; Tectronix Inc.) and amplified by homemade equipment. Figure 1(a) shows a schematic of the setup. This system provides a differential voltage of up to $\pm 24 \text{ V}$ at $\pm 200 \text{ mA}$ and an automatic shutdown circuit, which detects the drop-off of the wire and completion of the etching procedure^{12,14} by monitoring the power consumed by electrolysis \bar{P} and automatically shut down the voltage output

at \bar{P}_{SP} . The automatic shutdown circuit is widely used to prevent over-etching after the tip formation,^{12,14,22,23} which causes an increase in the tip radius.²³ In this experiment, we employed an architecture using a field effect transistor (FET) to eliminate the error of tip shape caused by the mechanical relay's delay.

The pattern of applied voltage is shown in Figure 1(b). This wave is obtained by modulating a fundamental sine wave of amplitude A and frequency f_0 with a sine wave of frequency f_s at modulation factor m . The following equation expresses the output voltage V_{out} versus time t .

$$V_{\text{out}}(t) = A \sin(2\pi f_0 t) \cdot \{1 + m \sin(2\pi f_s t)\} \quad (5)$$

The fabricated tips were investigated using a field emission (FE-) SEM (JSM-6500F; JEOL Inc.) equipped with EDX (JED-2300F; JEOL Inc.). Elemental distribution on the tip surface was also analyzed by APT using a local-electrode-type²⁴ instrument (Ametek, LEAP4000X HR) in voltage mode at the temperature of 50 K.

STM analysis was performed on cleaved HOPG (Highly oriented pyrolytic graphite, grade ZYB; purchased from Alliance Biosystems, Inc.) and Pt-deposited mica substrates in the air at room temperature. Pt (99.99 %; purchased from Furuuchi Chemical Corp.) was deposited on the cleaved surface of muscovite mica $[\text{KAl}_2(\text{Si}_3\text{Al})\text{O}_{10}(\text{OH})_2]$ substrates (purchased from Furuuchi Chemical Corp.) by electron beam evaporation in vacuum below 1×10^{-4} Pa at room temperature. AFM analysis was performed using a qPlus sensor²⁵⁻²⁸ built with a quartz tuning fork (QTF; purchased from SII Crystal Technology Inc.) and a fabricated Pt/Ir tip. The etched tip was cut into a length of ~ 1 mm and glued to the end of one prong of the QTF by epoxy resin (EPO-TEK H70E; Epoxy Technology Inc.), and the other prong was fixed to the mount. The KCl{100} surface in 1-methyl-1-propylpyrrolidinium bis(trifluoromethylsulfonyl)imide (Py_{1,3}-TF₂N) was used as the sample for the qPlus AFM analysis. The cleavage of the single crystal exposed the KCl{100} surface, and 0.5 μL of Py_{1,3}-TF₂N (99.5 %, purchased from IoLiTec GmbH) saturated with KCl (>99.5 %, Fujifilm Wako Pure Chemical Corp.) was dropped on the surface and settled for 24 h in the dry chamber before analysis. The STM and AFM analysis was performed by a system based on a commercial AFM/STM (JEOL Ltd., JSPM-5200) with a homebuilt STM head for small current detection and a homebuilt AFM head for qPlus sensor²⁷. AFM analysis was

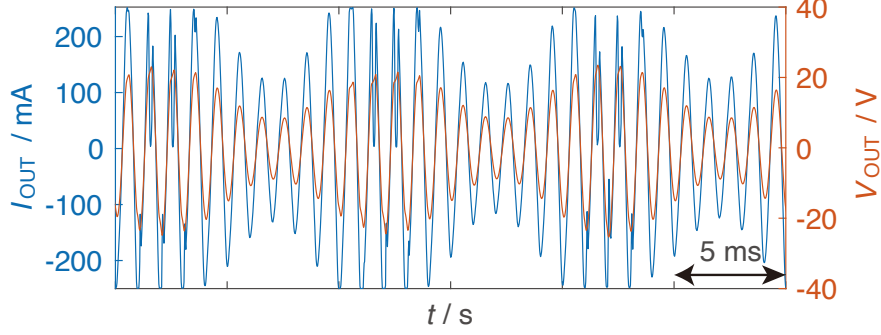


FIG. 2. The current I_{OUT} versus time t curve obtained in the middle of the etching procedure. $f_0 = 1000 \text{ Hz}$, $f_s = 100 \text{ Hz}$, $A = 18 \text{ V}$ and $m = 50 \%$.

performed in frequency modulation (FM) mode.²⁹ The instrument's configuration was the same as previously reported.^{30,31}

Figure 2 shows the current I_{OUT} and voltage V_{OUT} curves versus time t obtained during the etching procedure at $f_0 = 1000 \text{ Hz}$, $f_s = 100 \text{ Hz}$, $A = 18 \text{ V}$ and $m = 50 \%$. $I_{\text{OUT}} - t$ and $V_{\text{OUT}} - t$ curves for the entire etching time and around the shutdown operation are shown in Figure S1 in the supporting information. In the region where $|V_{\text{OUT}}|$ is approximately 14 V ($\sim 10 V_{\text{rms}}$) or higher, there is significant distortion in the $I_{\text{OUT}} - t$ curve, while it is almost negligible in the region where $|V_{\text{OUT}}| < 14 \text{ V}$. This suggests that the current was impeded by the bubbles or passivation film formation on the tip surface at high voltages of $|V_{\text{OUT}}| > 14 \text{ V}$, which did not occur at $|V_{\text{OUT}}| < 14 \text{ V}$. Considering that intense bubble generation was observed even when an amplitude $|V_{\text{OUT}}|$ of 14 V or less was applied, it is expected that anodic oxidation of Pt progressed only above 14 V , and that only flushing by gas bubbles occurred below 14 V . Note that the passive film can be formed not only by the oxidation of Pt but also by the precipitation of Pt particles coated with impurities¹² due to the reduction of the PtCl_x and PtO_x ¹⁸ on the tip surface or the reduction of $[\text{PtCl}_4]^{2-}$ and $[\text{PtCl}_6]^{2-}$ ions dissolved in the electrolyte. Therefore, it is reasonable that the $I_{\text{OUT}} - t$ curve shows distortions at high voltage in both anodic and cathodic reactions.

Figures 3(a-c) show SEM images of tips fabricated at $A = 18 \text{ V}$, $f_s = 100 \text{ Hz}$, $m = 50 \%$ and (a) $f_0 = 1000 \text{ Hz}$, (b) $f_0 = 2000 \text{ Hz}$ and (c) $f_0 = 900 \text{ Hz}$, respectively. For comparison, Figure 3(d) shows a tip fabricated without amplitude modulation (*i.e.* $m = 0$) at $A = 18 \text{ V}$ ($= 12.7 V_{\text{rms}}$) and $f_0 = 1000 \text{ Hz}$. As shown in Figure 3(a), a clean tip with a radius of curvature of 60 nm was obtained at $f_0 = 1000 \text{ Hz}$. At a higher frequency of $f_0 = 2000$

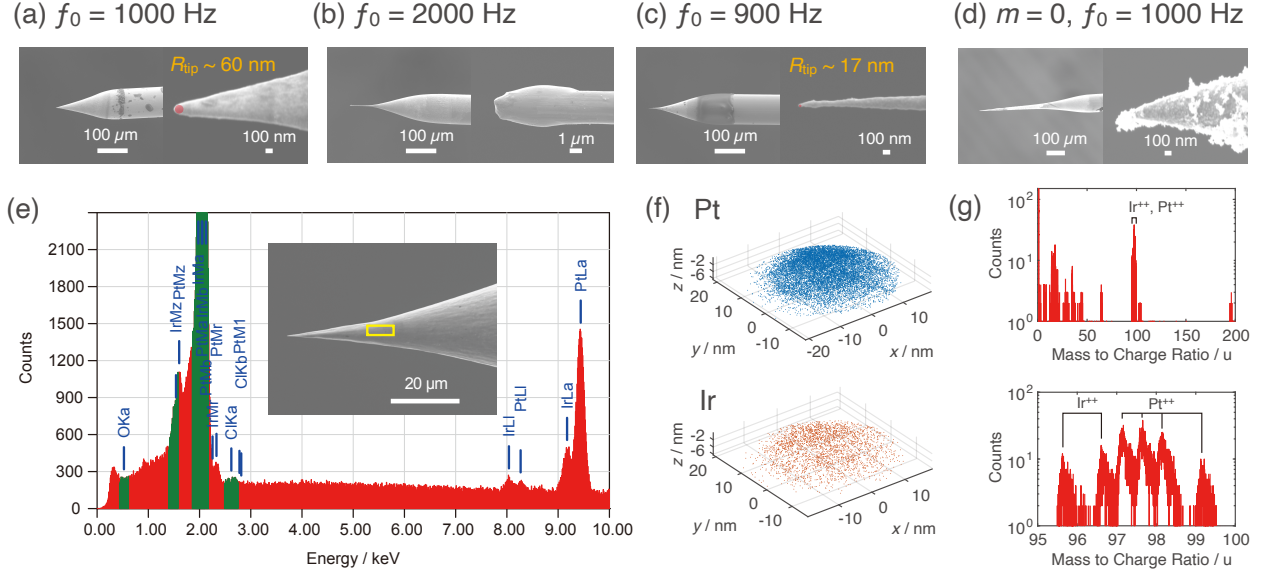


FIG. 3. (a-c) The SEM images of tips fabricated at $A = 18$ V, $f_s = 100$ Hz, $m = 50\%$ and (a) $f_0 = 1000$ Hz, (b) $f_0 = 2000$ Hz and (c) $f_0 = 900$ Hz, respectively. (d) The SEM image of a tip fabricated without amplitude modulation ($m = 50\%$) at $A = 18$ V and $f_0 = 1000$ Hz. (e) The EDX spectrum obtained at a tip surface fabricated at $A = 18$ V, $f_s = 100$ Hz, $m = 50\%$ and $f_0 = 1000$ Hz in the region marked by a yellow box in the SEM image. (f,g) The distribution map of Pt and Ir atoms (f) and corresponding histogram of mass-to-charge ratio (g) obtained by APT analysis of a tip fabricated at $A = 18$ V, $f_s = 100$ Hz, $m = 50\%$ and $f_0 = 1000$ Hz.

Hz, the tip shape tended to be irregular, as shown in Figure 3(b). This trend is similar to that already reported by Aoyama *et al.*¹⁷ on the multi-step AC electropolishing of Pt/Ir tips without amplitude modulation, where the radius of curvature increases at frequencies higher than 1 kHz.

Conversely, at a lower frequency of $f_0 = 900$ Hz, a smaller radius of curvature of 17 nm was obtained than at $f_0 = 1000$ Hz. However, more impurities were deposited on the tip surface, visualized as black shadows in the SEM images. This suggests that impurities are more likely to be deposited at lower frequencies, while the radius of curvature of the tip tends to be larger at higher frequencies. For this reason, we concluded that $f_0 = 1000$ Hz was the optimum frequency for obtaining a clean and sharp tip. Under these conditions, 12 tips were consecutively fabricated, and 67 % of the tips had a radius of curvature of less than 100 nm, as shown in Figure S2 in the supporting information.

For comparison, a tip was also fabricated without amplitude modulation. The relatively

sharp tips with a radius of curvature of less than 1 μm were obtained at $f_0 = 1000$ Hz, as shown in Figure 3(d). However, the tip was covered with a lot of impurities, and it was impossible to achieve both a small radius of curvature and a clean tip surface by adjusting the frequency with no amplitude modulation. This result also corresponds to the previous report¹⁷. Also, since it is known that a large amplitude tends to roughen the tip shape¹⁶, an amplitude much greater than $10 V_{\text{rms}}$, the minimum voltage required for the etching reaction, is not suitable for obtaining a tip with a small radius of curvature. Therefore, we can conclude that a clean and sharp tip cannot be achieved by simply adjusting amplitude or frequency and that amplitude modulation is the key to obtaining the clean and sharp Pt/Ir tips by AC electropolishing.

Figure 3(e) shows an EDX spectrum obtained at a tip surface. Hereafter, all analyses were performed with the tips fabricated by amplitude-modulated AC electropolishing with $f_0 = 1000$ Hz, $f_s = 100$ Hz, $A = 18$ V and $m = 50\%$. Only Pt and Ir peaks were intense, and O and Cl peaks were negligibly small. Note that a C peak found at 0.277 keV originates from carbon contamination³² during the SEM analysis. This result indicates that no oxides or chlorides were detected on the tip surface, suggesting a clean metal surface was exposed. In addition, the distribution of Pt and Ir atoms on the tip surface was analyzed by APT. Figure 3(f) shows the distribution maps for Pt and Ir atoms on the tip surface reconstructed from the detected positions and time of flight of the ionized atoms on the APT analysis.²⁰ The result shows that the Pt and Ir elements are homogeneously distributed on the tip surface. Figure 3(g) shows a histogram of mass-to-charge ratios corresponding to the areas analyzed in Figure 3(f). The approximate elemental compositions estimated from the area of Pt^{++} and Ir^{++} peaks shown in Figure 3(g) were 83 % for Pt and 17 % for Ir, which were close to those of the bulk.

Figure 4(a) shows the STM topographic image of a Pt-deposited mica substrate obtained using an amplitude-modulated-AC-etched Pt/Ir tip. The spherical grains were clearly imaged, and the line profiles obtained on the trace and retrace scans were overlapped entirely, suggesting that a stable scan was performed. We also carried out STM imaging on the Pt substrate using an as-cut Pt/Ir wire without etching for comparison, as shown in Figure 4(b). The deposited grains were imaged in a more distorted shape than those imaged by the etched tip, and the trace and retrace profiles showed a large discrepancy. This suggests that the irregular shape of the as-cut tip resulted in unstable scans and distorted images

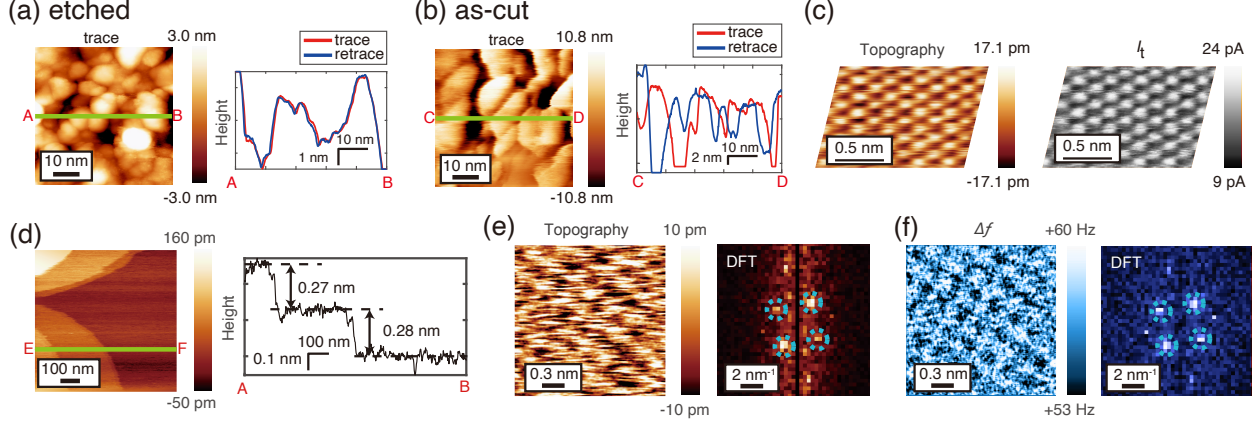


FIG. 4. (a, b) STM images and line profiles of Pt-deposited mica surface obtained using an (a) etched tip and (b) conventional as-cut wire. Bias Voltage= 511 mV and tunneling current $I_t \sim 1 \times 10^1$ pA. (c) STM topography (z) and tunneling current (I_t) images of the HOPG surface obtained using an etched tip. Bias Voltage= 68 mV. (d-f) qPlus AFM images obtained on KCl{100} surface in KCl-saturated Py_{1,3}-TF₂N. (d) large-area topography with line profiles, (e) high-resolution topography with its discrete Fourier transform (DFT) image, and (f) corresponding Δf image with its DFT image. $Q = 145$, $f = 18\,473$ Hz, $A_{p-p} \sim 3 \times 10^2$ pm.

with the tip artifact. In other words, although an as-cut tip has been applied to various STM analyses in air, including atomic-scale high-resolution analysis³³, an etched tip with a well-determined shape is especially advantageous for analyzing macroscopic features of highly rough surfaces. Also, a HOPG surface was imaged to demonstrate its applicability to high-resolution analysis. Figure 4(c) shows the topography and tunneling current (I_t) images obtained on the cleaved surface of HOPG. Both images show the well-known six-fold symmetry contrast which is consistent with the arrangement of β carbon atoms.^{34–36} This means that the etched tip provides a stable analysis even on the atomic scale and can replace the conventional as-cut tips in STM.

Furthermore, the fabricated tips were also applied to high-resolution FM-AFM analysis. Figure 4(d) shows a large-area topographic image of the KCl{100} surface and its line profile obtained by qPlus AFM in KCl-saturated Py_{1,3}-TF₂N. Atomically flat terraces and atomic steps with a height of ~ 0.27 nm were clearly imaged, where the obtained step height was close to the thickness of a single atomic layer on KCl{100} of 0.31 nm^{37,38}. Figures 4(d) and 4(e) show a high-resolution topographic image and the corresponding frequency-

shift (Δf) image obtained on the terrace surface, respectively. Although the signal-to-noise ratio is poorer than that reported using an electropolished W tip, both images show four-fold symmetric contrasts corresponding to the arrangement of K or Cl ions in KCl{100} surface³⁸, and the corresponding four bright spots are clearly shown in the discrete Fourier transform (DFT) image. This means that the resolution reaches the atomic scale for both the vertical and horizontal directions.

In summary, we developed a method to fabricate sharp and clean Pt/Ir tips by amplitude-modulated AC electropolishing. The clean tips with a radius of curvature less than 100 nm were reproducibly obtained at $f_0 = 1000$ Hz, $f_s = 100$ Hz, $A = 18$ V and $m = 50\%$. SEM-EDX and APT analyses showed that a uniform Pt/Ir alloy was exposed on the tip surface as a clean surface without O or Cl contamination. The STM imaging using the fabricated tip showed that it is more suitable for investigating rough surfaces than as-cut tips and applicable for atomic-resolution imaging. Furthermore, we applied the fabricated tip to qPlus AFM analysis in liquid and showed that it has atomic resolution in both the horizontal and vertical directions. Therefore, it is concluded that the amplitude-modulated AC etching method reproducibly provides sharp STM/AFM tips capable of both atomic resolution and large-area analyses without complex etching setups.

SUPPLEMENTARY MATERIAL

- Control of applied voltage by automatic shutdown circuit and the evaluation of the reproducibility of etched tips by consecutive fabrication.

ACKNOWLEDGMENTS

This work was supported by a Grant-in-Aid for Scientific Research B (JP23H01850) from the Japan Society for the Promotion of Science (JSPS).

AUTHOR DECLARATIONS

Conflict of Interest

The authors have no conflicts to disclose.

Author Contributions

Y.N. drafted the original paper. Y.N. developed the etching equipment and fabricated the sample tip. Y.N performed the STM, AFM, and SEM-EDX experiments. S.K. performed the APT experiment. T.I. developed the STM/AFM equipment and coordinated the project. T.U., S.K., and T.I. contributed to the interpretation of the results. All authors discussed the results and contributed to the preparation of the paper.

DATA AVAILABILITY STATEMENT

The data that support the findings of this study are available from the corresponding author upon reasonable request.

REFERENCES

- ¹J. Garnaes, F. Kragh, K. A. Mo/rch, and A. R. Thölén, “Transmission electron microscopy of scanning tunneling tips,” *Journal of Vacuum Science & Technology A: Vacuum, Surfaces, and Films* **8**, 441–444 (1990).
- ²K. Bian, C. Gerber, A. J. Heinrich, D. J. Müller, S. Scheuring, and Y. Jiang, “Scanning probe microscopy,” *Nature Reviews Methods Primers* **1**, 36 (2021).
- ³I. H. Musselman and P. E. Russell, “Platinum/iridium tips with controlled geometry for scanning tunneling microscopy,” *Journal of Vacuum Science & Technology A: Vacuum, Surfaces, and Films* **8**, 3558–3562 (1990).
- ⁴G. Binnig, H. Rohrer, C. Gerber, and E. Weibel, “Surface studies by scanning tunneling microscopy,” *Physical Review Letters* **49**, 57–61 (1982).
- ⁵B. L. Rogers, J. G. Shapter, W. M. Skinner, and K. Gascoigne, “A method for production of cheap, reliable pt-ir tips,” *Review of Scientific Instruments* **71**, 1702–1705 (2000).
- ⁶A. A. Gorbunov, B. Wolf, and J. Edelmann, “The use of silver tips in scanning tunneling microscopy,” *Review of Scientific Instruments* **64**, 2393–2394 (1993).
- ⁷M. Fotino, “Tip sharpening by normal and reverse electrochemical etching,” *Review of Scientific Instruments* **64**, 159–167 (1993).

- ⁸A. J. Melmed, “The art and science and other aspects of making sharp tips,” *Journal of Vacuum Science & Technology B: Microelectronics and Nanometer Structures Processing, Measurement, and Phenomena* **9**, 601–608 (1991).
- ⁹A. A. Gewirth, D. H. Craston, and A. J. Bard, “Fabrication and characterization of microtips for in situ scanning tunneling microscopy,” *J. Electroanal. Chem* **261**, 477–482 (1989).
- ¹⁰L. Libiouille, Y. Houbion, and J. M. Gilles, “Very sharp platinum tips for scanning tunneling microscopy,” *Review of Scientific Instruments* **66**, 97–100 (1995).
- ¹¹J. Zhang, Y. Gonzalez, R. Sany, and A. Ruediger, “A facile fabrication procedure for platinum nanoprobe with high-aspect-ratio and low tip radii via electrochemical etching,” *Review of Scientific Instruments* **91** (2020), 10.1063/1.5128653.
- ¹²T. Takami, R. Kitamura, T. Hiramoto, S. Oki, K. Yoshioka, and Y. Aoyama, “Automatic shutdown system of alternating current electrochemical etching for the preparation of a platinum/iridium tip for scanning tunneling microscopy and the investigation of the byproduct of platinum chloride particles,” *Japanese Journal of Applied Physics* **58**, SIIC05 (2019).
- ¹³M. Fotino, “Nanotips by reverse electrochemical etching,” *Applied Physics Letters* **60**, 2935–2937 (1992).
- ¹⁴J. A. Meza, J. Polesel-Maris, C. Lubin, F. Thoyer, A. Makky, A. Ouerghi, and J. Cousty, “Reverse electrochemical etching method for fabricating ultra-sharp platinum/iridium tips for combined scanning tunneling microscope/atomic force microscope based on a quartz tuning fork,” *Current Applied Physics* **15**, 1015–1021 (2015).
- ¹⁵J. Lindahl, T. Takanen, and L. Montelius, “Easy and reproducible method for making sharp tips of pt/ir,” *Journal of Vacuum Science & Technology B: Microelectronics and Nanometer Structures Processing, Measurement, and Phenomena* **16**, 3077–3081 (1998).
- ¹⁶A. H. Sørensen, U. Hvid, M. W. Mortensen, and K. A. Mørch, “Preparation of platinum/iridium scanning probe microscopy tips,” *Review of Scientific Instruments* **70**, 3059–3067 (1999).
- ¹⁷Y. Aoyama and T. Takami, “Frequency dependence of alternate current electrochemical etching of platinum/iridium wire,” *Research reports of Kogakuin University* **123**, 53–58 (2017).

- ¹⁸B. R. Shrestha, E. Tada, and A. Nishikata, “Effect of chloride on platinum dissolution,” *Electrochimica Acta* **143**, 161–167 (2014).
- ¹⁹R. S. Patil, V. A. Juvekar, and V. M. Naik, “Oxidation of chloride ion on platinum electrode: Dynamics of electrode passivation and its effect on oxidation kinetics,” *Industrial and Engineering Chemistry Research* **50**, 12946–12959 (2011).
- ²⁰A. Devaraj, D. E. Perea, J. Liu, L. M. Gordon, T. J. Prosa, P. Parikh, D. R. Diercks, S. Meher, R. P. Kolli, Y. S. Meng, and S. Thevuthasan, “Three-dimensional nanoscale characterisation of materials by atom probe tomography,” *International Materials Reviews* **63**, 68–101 (2018).
- ²¹G. Binnig, C. F. Quate, and C. Gerber, “Atomic force microscope,” *Physical Review Letters* **56**, 930–933 (1986).
- ²²I. V. Borzenets, I. Yoon, M. W. Prior, B. R. Donald, R. D. Mooney, and G. Finkelstein, “Ultra-sharp metal and nanotube-based probes for applications in scanning microscopy and neural recording,” *Journal of Applied Physics* **111**, 074703 (2012).
- ²³Y. Nakamura, Y. Mera, and K. Maeda, “A reproducible method to fabricate atomically sharp tips for scanning tunneling microscopy,” *Review of Scientific Instruments* **70**, 3373–3376 (1999).
- ²⁴T. F. Kelly and D. J. Larson, “Local electrode atom probes,” *Materials Characterization* **44**, 59–85 (2000).
- ²⁵F. J. Giessibl, “The qplus sensor, a powerful core for the atomic force microscope,” *Review of Scientific Instruments* **90**, 011101 (2019).
- ²⁶A. Auer, B. Eder, and F. J. Giessibl, “Electrochemical afm/stm with a qplus sensor: A versatile tool to study solid-liquid interfaces,” *Journal of Chemical Physics* **159**, 174201 (2023).
- ²⁷T. Ichii, M. Fujimura, M. Negami, K. Murase, and H. Sugimura, “Frequency modulation atomic force microscopy in ionic liquid using quartz tuning fork sensors,” *Japanese Journal of Applied Physics* **51**, 08KB08 (2012).
- ²⁸T. Ichii, M. Negami, and H. Sugimura, “Atomic-resolution imaging on alkali halide surfaces in viscous ionic liquid using frequency modulation atomic force microscopy,” *Journal of Physical Chemistry C* **118**, 26803–26807 (2014).
- ²⁹T. R. Albrecht, P. Grütter, D. Horne, and D. Rugar, “Frequency modulation detection using high-q cantilevers for enhanced force microscope sensitivity,” *Journal of Applied*

- Physics **69**, 668–673 (1991).
- ³⁰Y. Bao, Y. Nishiwaki, T. Kawano, T. Utsunomiya, H. Sugimura, and T. Ichii, “Molecular-resolution imaging of ionic liquid/alkali halide interfaces with varied surface charge densities via atomic force microscopy,” ACS Nano **18**, 25302–25315 (2024).
- ³¹Y. Nishiwaki, Y. Yamada, T. Utsunomiya, H. Sugimura, and T. Ichii, “Interfacial structures and mechanical response of highly viscous polymer melt on solid surfaces investigated by atomic force microscopy,” The Journal of Physical Chemistry C **128**, 11966–11976 (2024).
- ³²M. Hugenschmidt, K. Adrion, A. Marx, E. Müller, and D. Gerthsen, “Electron-beam-induced carbon contamination in stem-in-sem: Quantification and mitigation,” Microscopy and Microanalysis **29**, 219–234 (2023).
- ³³W.-T. Pong, J. Bendall, and C. Durkan, “Observation and investigation of graphite superlattice boundaries by scanning tunneling microscopy,” Surface Science **601**, 498–509 (2007).
- ³⁴Y. Wang, Y. Ye, and K. Wu, “Simultaneous observation of the triangular and honeycomb structures on highly oriented pyrolytic graphite at room temperature: An stm study,” Surface Science **600**, 729–734 (2006).
- ³⁵J. Schneir, R. Sonnenfeld, P. K. Hansma, and J. Tersoff, “Tunneling microscopy study of the graphite surface in air and water,” Physical Review B **34**, 4979–4984 (1986).
- ³⁶D. Tománek, S. G. Louie, H. J. Mamin, D. W. Abraham, R. E. Thomson, E. Ganz, and J. Clarke, “Theory and observation of highly asymmetric atomic structure in scanning-tunneling-microscopy images of graphite,” Physical Review B **35**, 7790–7793 (1987).
- ³⁷D. Walker, P. K. Verma, L. M. Cranswick, R. L. Jones, S. M. Clark, and S. Buhre, “Halite-sylvite thermoelasticity,” American Mineralogist **89**, 204–210 (2004).
- ³⁸G. Schwabegger, T. Djuric, H. Sitter, R. Resel, and C. Simbrunner, “Morphological and structural investigation of sexithiophene growth on kcl (100),” Crystal Growth and Design **13**, 536–542 (2013).

Supporting Information for “One-step Fabrication of Sharp Platinum/Iridium Tips via Amplitude-Modulated Alternating-Current Electropolishing”

Y. Nishiwaki, T. Utsunomiya, S. Kurokawa, and T. Ichii*

*Department of Materials Science and Engineering, Kyoto University,
Yoshida Honmachi, Sakyo, Kyoto, 606-8501, Japan.*

(*Electronic mail: ichii.takashi.2m@kyoto-u.ac.jp)

(Dated: 3 December 2024)

I. CONTROL OF APPLIED VOLTAGE BY AUTOMATIC SHUTDOWN CIRCUIT

Figure S1 shows the current I_{OUT} and voltage V_{OUT} curves versus time t obtained during etching procedure at $f_0 = 1000 \text{ Hz}$, $f_s = 100 \text{ Hz}$, $A = 18 \text{ V}$ and $m = 50 \%$. Figure S1(a) shows the $I_{\text{OUT}} - t$ curve for the entire etching time. I_{OUT} decreases during the etching procedure because the resistance increases as the etching and necking of the wire near the liquid surface progresses.^{1,2} Note that, even without a shutdown circuit, I_{OUT} and \bar{P} drop off at the end as the tip is formed. However, an automatic shutdown circuit is required to suppress the voltage application after the drop-off of the current to prevent over-etching after tip formation and reduce the radius of the curvature of the tip, as mentioned in the main text.

The automatic shutdown circuit calculated the effective power \bar{P} by smoothing the instantaneous power with an 8th-order Bessel low-pass filter with a cutoff frequency of $f_{\text{LPF}} = 704 \text{ Hz}$. It shut down the voltage output when \bar{P} became less than $\bar{P}_{\text{SP}} \sim 0.10 \text{ W}$. Figure S1(b) shows the I_{OUT} and V_{OUT} versus t curves at the end of the etching. The V_{OUT} was shut down at the end of etching in the fall time within $50 \mu\text{s}$, which is sufficiently smaller than the operating time or the release time of a conventional mechanical relay. The voltage fluctuation after the shutdown was less than $0.3 V_{\text{p-p}}$, which was small enough to stop the anodization and gas generation reaction.

II. EVALUATION OF THE REPRODUCIBILITY OF ETCHED TIPS BY CONSECUTIVE FABRICATION

Figure S2 shows SEM images and radius of curvature R_{tip} of a series of tips fabricated in a single bath. Except for Tip 9, the tips have a radius of curvature less than 300 nm , of which 67% have a radius less than 100 nm . The round shape in Tip 9 may have been caused by the melting by Joule heating,³ which was sometimes observed regardless of the times the bath was used. On the surface of Tip 12, despite the small radius of curvature, a black precipitate was deposited on the shoulder of the tip shank, which appeared as a shadow on the SEM image. At this time, the bath was contaminated by black dispersed particles of Pt and PtCl_x , and the viscosity was increased by the evaporation of acetone,

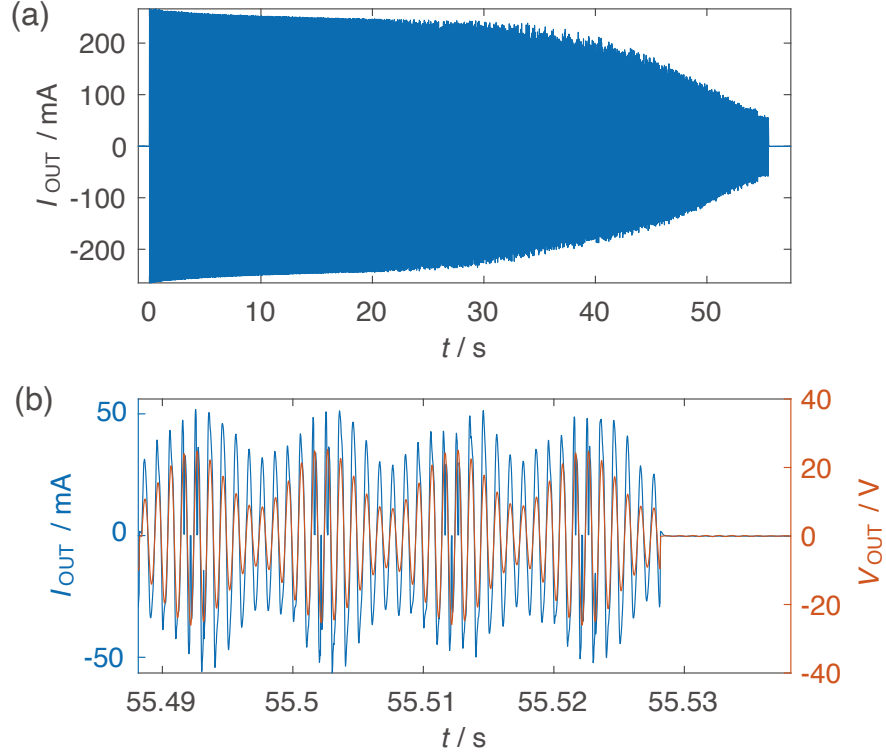


FIG. S1. (a) The current I_{OUT} versus time t curve obtained for entire etching time. (b) The current I_{OUT} and voltage V_{OUT} versus time t curves obtained at the end of the etching procedure. $f_0 = 1000\text{ Hz}$, $f_s = 100\text{ Hz}$, $A = 18\text{ V}$ and $m = 50\%$.

which probably prevented sufficient removal of the deposits on the tip surface. Therefore, the lifetime of the electrolyte is limited to approximately 12 cycles, within which a clean tip with a radius of curvature of less than 100 nm can be obtained with a production yield rate of approximately 67 %.

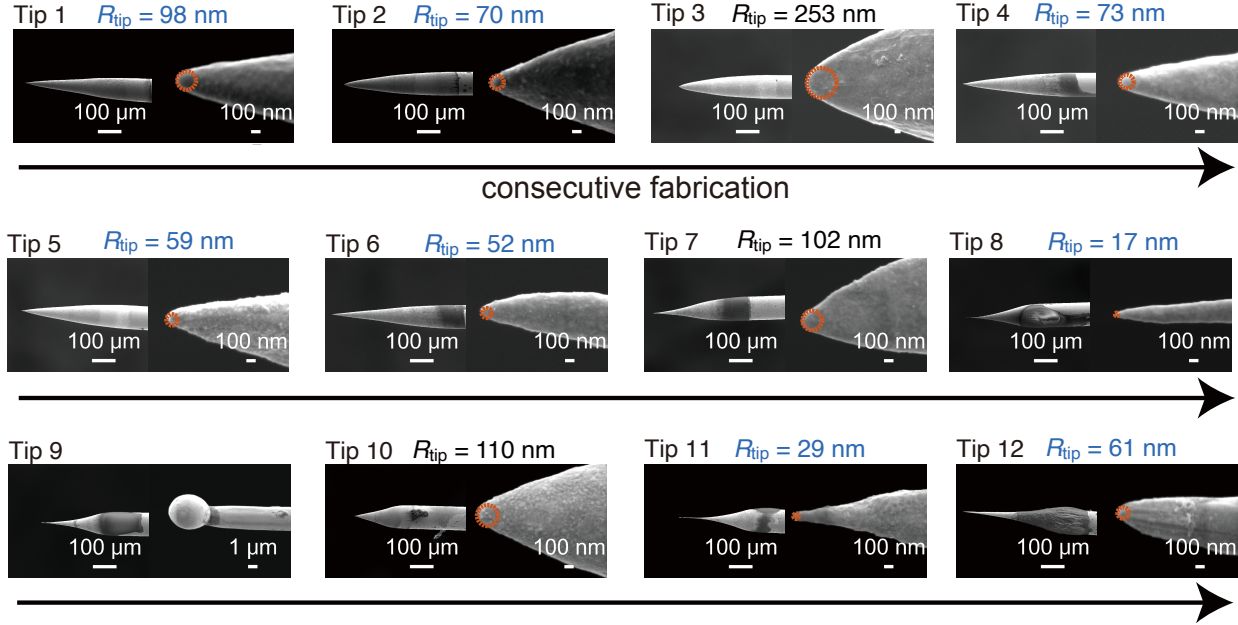


FIG. S2. SEM images and radii of curvature R_{tip} of a series of tips fabricated in a single bath.

REFERENCES

- ¹L. Libiouille, Y. Houbion, and J. M. Gilles, “Very sharp platinum tips for scanning tunneling microscopy,” *Review of Scientific Instruments* **66**, 97–100 (1995).
- ²T. Takami, R. Kitamura, T. Hiramoto, S. Oki, K. Yoshioka, and Y. Aoyama, “Automatic shutdown system of alternating current electrochemical etching for the preparation of a platinum/iridium tip for scanning tunneling microscopy and the investigation of the byproduct of platinum chloride particles,” *Japanese Journal of Applied Physics* **58**, SIIC05 (2019).
- ³A. H. Sørensen, U. Hvid, M. W. Mortensen, and K. A. Mørch, “Preparation of platinum/iridium scanning probe microscopy tips,” *Review of Scientific Instruments* **70**, 3059–3067 (1999).